von Schiller Daniel (Orcid ID: 0000-0002-9493-3244)
Datry Thibault (Orcid ID: 0000-0003-1390-6736)
Marce Rafael (Orcid ID: 0000-0002-7416-4652)
García-Baquero Gonzalo (Orcid ID: 0000-0001-6550-1584)
Odriozola Iñaki (Orcid ID: 0000-0002-5289-7935)
Obrador Biel (Orcid ID: 0000-0003-4050-0491)
Mendoza-Lera Clara (Orcid ID: 0000-0002-3222-2498)
Arnon Shai (Orcid ID: 0000-0002-7109-8979)
Boëchat Iola, G (Orcid ID: 0000-0002-9651-6364)
Bond Nick, R (Orcid ID: 0000-0003-4294-6008)
Burrows Ryan (Orcid ID: 0000-0002-3296-1864)
Cauvy-Fraunié Sophie (Orcid ID: 0000-0001-8600-0519)
De Girolamo Anna, M (Orcid ID: 0000-0001-5605-6239)
del Campo Rubén (Orcid ID: 0000-0002-0560-831X)
Figueroa Ricardo (Orcid ID: 0000-0003-2715-5275)
Gómez-Gener Lluís (Orcid ID: 0000-0003-3279-3589)
Guareschi Simone (Orcid ID: 0000-0003-2962-0863)
Gücker Björn (Orcid ID: 0000-0002-0884-8650)
Langhans Simone, Daniela (Orcid ID: 0000-0001-9581-3183)
Leigh Catherine (Orcid ID: 0000-0003-4186-1678)
McIntosh Angus (Orcid ID: 0000-0003-2696-8813)
Mlambo Musa, C (Orcid ID: 0000-0001-7624-5686)
Morais Manuela (Orcid ID: 0000-0003-0482-4309)
Negus Peter (Orcid ID: 0000-0003-2680-2573)
Pardo Isabel (Orcid ID: 0000-0002-4553-1310)
Rolls Robert, J (Orcid ID: 0000-0002-0402-411X)
Vander Vorste Ross (Orcid ID: 0000-0003-3423-5644)
Woelfle-Erskine Cleo (Orcid ID: 0000-0002-4363-237X)
Zak Dominik (Orcid ID: 0000-0002-1229-5294)

Sediment Respiration Pulses in Intermittent Rivers and Ephemeral Streams

D. von Schiller[1], T. Datry[2], R. Corti[2,3], A. Foulquier[4], K. Tockner[3,5], R. Marcé[6], G. García-Baquero[1], I. Odriozola[1,7], B. Obrador[8], A. Elosegi[1], C. Mendoza-Lera[2], M. O. Gessner[3,9], R. Stubbington[10], R. Albariño[11], D. C. Allen[12], F. Altermatt[13,52], M. I. Arce[3,14], S. Arnon[15], D. Banas[16], A. Banegas-Medina[17], E. Beller[18], M. L. Blanchette[19], J. F. Blanco-Libreros[20], J. Blessing[21], I. G. Boëchat[22], K. S. Boersma[23], M. T. Bogan[24], N. Bonada[25], N. R. Bond[26], K. Brintrup[17], A. Bruder[27], R. M. Burrows[28], T. Cancellario[29], S. M. Carlson[30], S. Cauvy-Fraunié[2], N. Cid[25], M. Danger[31], B. de Freitas Terra[32], A. Dehedin[33], A. M. De Girolamo[34], R. del Campo[3,35], V. Díaz-Villanueva[36], C. P.

This article has been accepted for publication and undergone full peer review but has not been through the copyediting, typesetting, pagination and proofreading process which may lead to differences between this version and the Version of Record. Please cite this article as doi: 10.1029/2019GB006276

© 2019 American Geophysical Union. All rights reserved.

Accepted Article

Duerdoth[37], F. Dyer[38], E. Faye[39], C. Febria[40,41], R. Figueroa[17], B. Four[42], S. Gafny[43], R. Gómez[35], Ll. Gómez-Gener[44], M. A. S. Graça[45], S. Guareschi[35,†], B. Gücker[22], F. Hoppeler[46], J. L. Hwan[30], S. Kubheka[47], A. Laini[48], S. D. Langhans[49,50], C. Leigh[28,51], C.J. Little[13,52], S. Lorenz[53], J. Marshall[21], E. J. Martín[52], A. McIntosh[40], E. I. Meyer[54], M. Miliša[55], M. C. Mlambo[56], M. Moleón[57], M. Morais[58], P. Negus[21], D. Niyogi[59], A. Papatheodoulou[60], I. Pardo[61], P. Pařil[62], V. Pešić[63], C. Piscart[64], M. Polášek[62], P. Rodríguez-Lozano[30], R. J. Rolls[65], M. M. Sánchez-Montoya[35], A. Savić[66], O. Shumilova[3,67,68], A. Steward[21], A. Taleb[69], A. Uzan[70], R. Vander Vorste[30], N. Waltham[71], C. Woelfle-Erskine[72] D. Zak[3,73,74], C. Zarfl[75], A. Zoppini[34]

[1] Department of Plant Biology and Ecology, Faculty of Science and Technology, University of the Basque Country (UPV/EHU), Bilbao, Spain.
[2] IRSTEA, UR RiverLY, Centre de Lyon-Villeurbanne, France.
[3] Leibniz-Institute of Freshwater Ecology and Inland Fisheries (IGB), Berlin, Germany.
[4] Université Grenoble Alpes, Laboratoire d'Écologie Alpine (LECA), UMR CNRS-UGA-USMB, Grenoble, France.
[5] Austrian Science Fund (FWF), Vienna, Austria.
[6] Catalan Institute for Water Research (ICRA), Girona, Spain.
[7] Laboratory of Environmental Microbiology, Institute of Microbiology of the CAS, Prague, Czech Republic.
[8] Department of Evolutionary Biology, Ecology and Environmental Sciences, University of Barcelona, Barcelona, Spain.
[9] Department of Ecology, Berlin Institute of Technology (TU Berlin), Berlin, Germany.
[10] School of Science and Technology, Nottingham Trent University, Nottingham, UK.
[11] INIBIOMA, Universidad Nacional del Comahue – CONICET, Bariloche, Argentina.
[12] Department of Biology, University of Oklahoma, Norman, OK, USA.
[13] Department of Evolutionary Biology and Environmental Studies, University of Zurich, Zürich, Switzerland.
[14] Centre of Edaphology and Applied Biology of Segura (CEBAS-CSIC), Murcia, Spain.
[15] Zuckerberg Institute for Water Research, The Jacob Blaustein Institutes for Desert Research, Ben-Gurion University of the Negev, Beersheba, Israel.
[16] Université de Lorraine - UR AFPA, Vandoeuvre-Les-Nancy, France.
[17] Faculty of Environmental Science, Centre of Environmental Science EULA Chile and CHRIAM Centre, Universidad de Concepción, Concepción, Chile.
[18] Department of Geography, University of California, Berkeley, CA, USA.
[19] Mine Water and Environment Research Centre (MiWER), School of Science, Edith Cowan University, Perth, Australia.
[20] Instituto de Biología (ELICE-RESTORES), Universidad de Antioquia, Medellín, Colombia.
[21] Department of Environment and Science, Queensland Government, Brisbane, Queensland, Australia.
[22] Department of Geosciences, Federal University of São João del-Rei, São João del-Rei, Brazil.
[23] Department of Biology, University of San Diego, San Diego, CA, USA.
[24] School of Natural Resources and the Environment, University of Arizona, Tucson, AZ, USA.

© 2019 American Geophysical Union. All rights reserved.

[25] Freshwater Ecology, Hydrology and Management (FEHM-Lab), Department of Evolutionary Biology, Ecology and Environmental Sciences, Institut de Recerca de la Biodiversitat (IRBio), University of Barcelona, Barcelona, Spain.
[26] Centre for Freshwater Ecosystems, La Trobe University, Wodonga, Victoria, Australia.
[27] Laboratory of Applied Microbiology, University of Applied Sciences and Arts of Southern Switzerland, Bellinzona, Switzerland.
[28] Australian Rivers Institute, Griffith University, Nathan, Queensland, Australia.
[29] University of Navarra, Biodiversity Data Analytics and Environmental Quality Group, Department of Environmental Biology, Pamplona, Spain.
[30] Department of Environmental Science, Policy, and Management, University of California, Berkeley, CA, USA.
[31] Université de Lorraine, LIEC, Metz, France.
[32] Centro de Ciências Agrárias e Biológicas, Universidade Estadual Vale do Acaraú, Sobral, Brazil.
[33] ASCONIT Consultants - Parc Scientifique Tony, Espace Henry Vallée, Lyon, France.
[34] Water Research Institute, National Research Council (IRSA-CNR), Montelibretti, Rome, Italy.
[35] Department of Ecology and Hydrology, Regional Campus of International Excellence 'Campus Mare Nostrum', University of Murcia, Murcia, Spain.
[36] INIBIOMA-CONICET, Bariloche, Argentina.
[37] Queen Mary University of London, River Laboratory, East Stoke, Wareham, UK.
[38] Institute for Applied Ecology, University of Canberra, Bruce, Australian Capital Territory, Australia.
[39] Centre International de Recherche en Agronomie pour le Développement, CIRAD, UPR HORTSYS, Montpellier, France.
[40] School of Biological Sciences, University of Canterbury, Christchurch, New Zealand.
[41] Great Lakes Institute for Environmental Research, University of Windsor, Windsor, Ontario, Canada.
[42] INRA, UAR 1275 DEPT EFPA, Centre de recherche de Nancy, Champenoux, France.
[43] Ruppin Academic Center, Michmoret, Israel.
[44] Department of Ecology and Environmental Science, Umeå University, Umeå, Sweden.
[45] MARE – Marine and Environmental Sciences Centre, Department of Life Sciences, University of Coimbra, Coimbra, Portugal.
[46] Senckenberg Biodiversity and Climate Research Centre (BiK-F), Frankfurt am Main, Germany.
[47] Ezemvelo KZN Wildlife, Pietermaritzburg, South Africa.
[48] Department of Chemistry, Life Sciences and Environmental Sustainability, University of Parma, Parma, Italy.
[49] University of Otago, Department of Zoology, Dunedin, New Zealand.
[50] BC3-Basque Centre for Climate Change, Leioa, Spain.
[51] Institute for Future Environments and ARC Centre of Excellence for Mathematical and Statistical Frontiers, School of Mathematics and Statistics, Science and Engineering Faculty, Queensland University of Technology, Brisbane, Australia.
[52] Department of Aquatic Ecology, Eawag, the Swiss Federal Institute of Aquatic Science and Technology, Dübendorf, Switzerland.
[53] Institute for Ecological Chemistry, Plant Analysis and Stored Product Protection, Julius-Kuehn-Institute, Berlin, Germany.
[54] Institute for Evolution and Biodiversity, Department of Limnology, University of Münster, Münster, Germany.
[55] Department of Biology, Faculty of Science, University of Zagreb, Zagreb, Croatia.

© 2019 American Geophysical Union. All rights reserved.

[56] Department of Freshwater Invertebrates, Albany Museum, Rhodes University Research Affiliated Institute, Grahamstown, South Africa.
[57] Department of Zoology, University of Granada, Granada, Spain.
[58] University of Évora, Évora, Portugal.
[59] Missouri University of Science and Technology, Rolla, MO, USA.
[60] Terra Cypria - The Cyprus Conservation Foundation, Limassol, Cyprus.
[61] Departamento de Ecología y Biología Animal, Universidad de Vigo, Vigo, Spain.
[62] Department of Botany and Zoology, Faculty of Science, Masaryk University, Brno, Czech Republic.
[63] Department of Biology, University of Montenegro, Podgorica, Montenegro.
[64] Univ Rennes, CNRS, ECOBIO UMR 6553, Rennes, France.
[65] School of Environment and Rural Science, University of New England, Armidale, New South Wales, Australia.
[66] Department of Biology and Ecology, Faculty of Sciences and Mathematics, University of Niš, Niš, Serbia.
[67] Freie Universität Berlin (FU), Institute of Biology, Berlin, Germany.
[68] Department of Civil, Environmental and Mechanical Engineering, Trento University, Trento, Italy.
[69] Laboratoire d'Écologie et Gestion des Ecosystèmes Naturels (LECGEN), University of Tlemcen, Tlemcen, Algeria.
[70] Nature and Parks Authority of Israel, Jerusalem, Israel.
[71] Centre for Tropical Water and Aquatic Ecosystem Research (TropWATER), College of Science and Engineering, James Cook University, Townsville, Queensland, Australia.
[72] School of Marine and Environmental Affairs, University of Washington, Seattle, WA, USA.
[73] University of Rostock, Institute of Landscape Ecology and Site Evaluation, Rostock, Germany.
[74] Aarhus University, Department of Bioscience, Silkeborg, Denmark.
[75] Center for Applied Geosciences, Eberhard Karls University of Tübingen, Germany.

Corresponding author: Daniel von Schiller (d.vonschiller@ehu.eus)

[†]Current address: Geography and Environment, Loughborough University, Loughborough, Leicestershire, UK.

Key Points:

- Sediment respiration in intermittent rivers and ephemeral streams increases substantially in response to rewetting
- Respiration pulses are driven by sediment properties, which, in turn, are influenced by climate and catchment characteristics
- Effects of wetting-drying cycles on respiration and CO_2 emissions in stream networks need consideration in upscaling and modeling efforts

© 2019 American Geophysical Union. All rights reserved.

Accepted Article

Abstract

Intermittent rivers and ephemeral streams (IRES) may represent over half the global stream network, but their contribution to respiration and carbon dioxide (CO_2) emissions is largely undetermined. In particular, little is known about the variability and drivers of respiration in IRES sediments upon rewetting, which could result in large pulses of CO_2. We present a global study examining sediments from 200 dry IRES reaches spanning multiple biomes. Results from standardized assays show that mean respiration increased 32–66-fold upon sediment rewetting. Structural equation modelling indicates that this response was driven by sediment texture and organic matter quantity and quality, which, in turn, were influenced by climate, land use and riparian plant cover. Our estimates suggest that respiration pulses resulting from rewetting of IRES sediments could contribute significantly to annual CO_2 emissions from the global stream network, with a single respiration pulse potentially increasing emission by 0.2–0.7%. As the spatial and temporal extent of IRES increases globally, our results highlight the importance of recognizing the influence of wetting-drying cycles on respiration and CO_2 emissions in stream networks.

1 Introduction

Most streams are heterotrophic ecosystems that act as net mineralizers of organic carbon (OC) and emit large quantities (0.56–1.8 Pg C yr^{-1}) of carbon dioxide (CO_2) to the atmosphere (Aufdenkampe et al., 2011; Raymond et al., 2013). A major limitation of current estimates of the influence of stream networks on global C cycling is their exclusion of intermittent rivers and ephemeral streams (IRES), which cease to flow and dry at some points in space and time (Acuña et al., 2014; Datry et al., 2018). IRES may represent over half of the global stream network length (Acuña et al., 2014) and are increasing in extent due to the combined effects of climate change, water abstraction, and land use change (Döll & Schmied, 2012; Pumo et al., 2016). Despite their prevalence, the role of IRES in C budgets of stream networks, including their contribution to respiration and CO_2 emission, is largely unknown (Datry et al., 2018; Marcé et al., 2019).

The hydrological regimes of IRES are characterized by alternating dry and wet phases, which exert a strong influence on C cycling (Datry et al., 2018; Marcé et al., 2019). Recent studies indicate that the effects of drying and rewetting on C mineralization in IRES sediments are similar to those in soils (Arce et al., 2019; Gallo et al., 2013; Marcé et al., 2019). Rewetting of dry IRES sediments through rain, groundwater upwelling or surface flow resumption may represent a respiration 'hot moment' (McClain et al., 2003) or 'control point' (Bernhardt et al., 2017) similar to the 'Birch effect' described in soils, resulting in large pulses of CO_2 compared to both the preceding dry phase and the subsequent extended flowing phase (Gallo et al., 2013; Marcé et al., 2019). Accordingly, a study addressing the effect of rewetting on CO_2 emissions from IRES sediments of the semiarid southwestern USA reported some of the largest flux increases ever observed in rewetting experiments(Gallo et al., 2013). Such CO_2 pulses could have considerable implications for stream network C budgets (Datry et al., 2018; Marcé et al., 2019). However, available data are restricted to few sites, limiting our ability to determine the variability and drivers of respiration in IRES and thus to upscale CO_2 emissions and include IRES in global biogeochemical models.

Here, we present a global research collaboration that collected and analyzed sediments from 200 dry IRES reaches across 29 countries, encompassing a wide range of conditions found in IRES worldwide (Figure 1; Table 1; Data file S1). We assessed the immediate effect of rewetting on sediment respiration using standardized assays and

© 2019 American Geophysical Union. All rights reserved.

estimated its potential influence on CO_2 emissions from stream networks. We predicted that, analogous to soils, dry IRES sediments would experience substantial increases in respiration upon rewetting. We further predicted that the magnitude of the effect would be a direct function of sediment characteristics such as texture and OC and nutrient content (proximal drivers), which in turn would depend on catchment characteristics such as climate, land use, and riparian plant cover (distal drivers).

2. Materials and Methods

2.1. Experimental Design

This coordinated experiment was conducted by contributors to the "1000 Intermittent Rivers Project" global research network (https://1000_intermittent_rivers_project.irstea.fr/). The collaborating research teams followed a standardized protocol (available on the website) to collect sediments and measure complementary environmental variables from a total of 200 IRES reaches during dry phases in the years 2015 and 2016. Despite the unparalleled global coverage of IRES in our experiment, gaps in spatial coverage exist due to a lack of contributors from some areas (e.g., large parts of Asia) or scarcity of IRES (e.g., in the boreal biome). Contributors were drawn from professional relationships and research networks and by responses to invitations posted on Twitter, Facebook and websites of professional organizations.

2.2. Sediment Sampling

The length of each sampled stream reach was defined as 10 times the average active channel width, to cover a representative area and to ensure consistent sampling effort (Leopold, 1966). The active channel was defined as the area of inundated and exposed streambed sediments between established edges of terrestrial vegetation, abrupt changes in slope, or both (Gordon et al., 2004). Within each reach, 5% of the streambed was randomly sampled within 1 m^2 quadrats (for example, five quadrats in a 100 m^2 reach). Streambed sediment samples were collected from each quadrat using a spoon or shovel to a depth of 10 cm and pooled into one composite sample of ~3 L in total across the sampled stream reach. In the laboratory, sediments were sieved (2 mm) and airdried for one week. A homogenized subsample of ~160 g was packed airtight in plastic containers and sent to the University of the Basque Country (Bilbao, Spain) for analysis. Upon arrival, samples were immediately stored at room temperature in the dark.

2.3. Environmental Variables

The active channel width (m) was determined by establishing 5–10 transects along each sampled stream reach. Riparian plant cover (%) was estimated by averaging the measurements obtained with a spherical densiometer or by visual assessment at each of the transects. Latitude and longitude (WGS 84 datum) of the sampling sites were determined with a global positioning system in the field or with a geographic information system (GIS). The proportion of the catchment area covered by agricultural and urban land uses (%) was determined using GIS based on the most updated national land cover maps. Results from GIS analyses were verified and corrected, if necessary, using ground-based surveys. Mean annual temperature (ºC) and precipitation (mm) were estimated based on the worldclim 2.0. database (http://www.worldclim.org), which gives 1-km^2 spatial resolution climate surfaces for global land areas over the period 1970–2000.

2.4. Sediment Characteristics

© 2019 American Geophysical Union. All rights reserved.

The OC and total nitrogen (N) content (%) of the sediments were determined using an elemental analyzer (TruSpec Micro CHNS, Leco Corp., St. Joseph, MI, USA) after grinding and acidification with 2M HCl. Analyses were run in duplicate. The C/N ratio is reported as the molar ratio of OC to N content. Clay content (% sediment particles <2 μm), a measure of sediment texture, was determined with a laser light diffraction instrument (Coulter LS 230, Beckman-Coulter, USA) after removing organic matter with H_2O_2 (Arriaga et al., 2006). Clay content is the main contributor to sediment permeability and sediment-specific area (Bear, 1988) which determine the area available for microbial colonization (Mendoza-Lera et al., 2017). Sediment water content, determined by weighing a subsample before and after oven drying (60ºC, 72 h), was low (mean ± SE = 1.7 ± 0.1%, median = 1.1, range = 0.1–15) and uncorrelated with sediment respiration change upon rewetting (Code S1).

2.5. Sediment Respiration Assays

Sediment respiration was measured in the laboratory under standardized conditions, which enabled us to compare intrinsic differences among sediments. Two different methods were used to ensure robust results. In dry conditions, we measured respiration using the commercial MicroResp™ device (Macaulay Scientific Consulting Ltd., UK), whereas in wet conditions, we measured respiration both with the MicroResp™ system and by determining the decline of dissolved oxygen (DO) concentrations in sealed incubation bottles.

For MicroResp™ measurements, 0.5 g of sediment was weighed into a deep well of an autoclaved 96 well microtiter plate. Samples were acclimated for 24 h at the temperature used later for the measurements (20ºC), and the incubation chamber was gently flushed with air to ensure that the partial pressure of CO_2 in the headspace of the wells was initially close to the atmospheric value (ca. 400 ppmv). For each sample, three analytical replicates were left in dry conditions and three were rewetted with 50 μL of air-saturated Volvic® mineral water immediately before covering and sealing the microtiter plate with a second microplate containing a CO_2 detection gel in the wells. We included controls consisting of empty wells and wells filled with 0.5 g of combusted and acid-washed glass beads (both with and without 50 μL of water added). Replicates and controls were randomized in the plates. The plates were incubated for 6 h at 20ºC, and the CO_2 molar fraction in each well's headspace was recorded immediately before and after the incubation by reading the absorbance of the detection gel in the microplate at 570 nm using a spectrophotometric microplate reader (BioTek EPOCH, Winooski, VT, USA). Because we used 26 different MicroResp™ plates for the whole experiment, we tested for any plate effects by duplicating the measurements of 18 samples in two different plates and found no significant differences. The mean error was 1.05 nmol CO_2 g^{-1} dry mass h^{-1} for dry samples and 7.15 nmol CO_2 g^{-1} dry mass h^{-1} for rewetted samples. Moreover, a linear mixed model of the whole dataset for CO_2 production in the wells including *plate* as a random factor allocated zero variability to the *plate* factor. Finally, the percentage change of CO_2 in the headspace was converted to a respiration rate (nmol CO_2 g^{-1} dry mass h^{-1}) considering the incubation time and temperature, gas constant, headspace volume and sediment mass, as described in the MicroResp™ technical manual. The mean values of the analytical replicates were used in further data analyses.

For the measurements of DO decline over time, we used two analytical replicates of 5 g aliquots per sediment sample and three controls without sediment for each of 10 successive runs comprising 25–50 samples. Samples and controls were introduced in acid-washed 250 mL glass incubation bottles filled with air-saturated Volvic® mineral water and sealed airtight using a 3.2-mm-thick silicon-PTFE septum and a cut-out open-top cap. Care was taken to ensure that air bubbles were excluded. Samples were incubated for 24 h at 20°C in an incubation chamber with gentle shaking (100 rpm, Multitron standard, INFORS HT,

© 2019 American Geophysical Union. All rights reserved.

Bottmingen, Switzerland). DO concentrations were measured at the end of the incubation with a DO microsensor (Microx 4 DO meter with a needle-type microsensor, PreSens, Regensburg, Germany) using a standalone, portable, fiberoptic DO meter (Microx 4 trace, PreSens). The incubation bottles were gently agitated before each measurement to ensure homogeneous DO concentrations. The DO decline (computed as the DO concentration difference between the control mean and the sample at the end of the incubation) was converted to CO_2 production (nmol CO_2 g^{-1} dry mass h^{-1}) based on a respiratory quotient of one. The mean values of analytical replicates were used in further data analyses.

To examine the response of sediment respiration to rewetting, we subtracted the respiration values in dry conditions (MicroResp™ dry) from those of the MicroResp™ and bottle incubations in wet conditions.

2.6. Potential Contribution to CO_2 Emissions from the Global Stream Network

To obtain an estimate of the potential contribution of respiration in IRES sediments upon rewetting to CO_2 emissions from the global stream network, we scaled up our results from the bottle incubations, assuming that i) all CO_2 produced and released by sediment respiration was emitted to the atmosphere, ii) sediment density averaged 1.6 g cm^{-3} across all sampled stream reaches (Hillel, 1980), and iii) the sediment depth potentially affected by a rewetting event was 30 cm, following common definitions of homogenous topsoils (Pistocchi et al., 2008). The obtained areal release rate was multiplied by the global annual accumulated dry area of IRES (84,461 km^2) estimated by Raymond et al., (2013). We considered one rewetting event with an effect duration of 5 days, following the mean duration of increased CO_2 flux in soils after rewetting estimated by Kim et al., (2012).

2.7. Statistical Analyses

All statistical analyses were conducted in R 3.4.0 (R Core Team, 2016). First, we tested for differences among the three measures of sediment respiration (MicroResp™ dry, MicroResp™ wet, and bottle incubations). The null hypothesis of no effect of rewetting on sediment respiration was tested with a randomized complete block ANOVA and Tukey's HSD post hoc test, using *site* as blocking factor and *method* as fixed explanatory factor (Code S1). The analysis was conducted on rank-transformed data to deal with heteroscedasticity in the residuals. Second, we tested the relationship between sediment respiration changes upon rewetting measured by the MicroResp™ and the bottle incubation method by fitting a Gaussian linear model using the function gls() in the R package *nlme* (Pinheiro et al., 2016). Adequate homoscedasticity in regression residuals was achieved by square-root transformation of both variables. The function gls() argument for modelling residual spatial autocorrelation included an exponential variogram model of the X (latitude) + Y (longitude) form, which was empirically shown to be appropriate to fulfil the model assumption of independence (Code S1). To assess whether the bottle incubation method overestimated sediment respiration change upon rewetting compared to the MicroResp™ method, we also tested the null hypothesis that β, the slope of the regression line, is $\beta = 1$ (rather than the null hypothesis that $\beta \neq 0$).

To model the causal relationships between environmental drivers and sediment respiration change upon rewetting, we used structural equation modelling (SEM) following the guidelines proposed in Grace et al. (2012), which allows the study of complete causal networks. The first step of the SEM approach was to devise a metamodel (Figure 2) (Grace et al., 2012), defined based on a priori theoretical knowledge and insights from the exploratory data analysis. . In this metamodel, we considered sediment respiration upon rewetting to be directly controlled by proximal drivers associated with sediment characteristics, which in turn

© 2019 American Geophysical Union. All rights reserved.

depend on distal drivers linked to catchment characteristics. For proximal drivers, we selected clay content as a measure of sediment texture, and OC content and the C/N ratio to indicate organic matter quantity and quality, respectively (Figure 2). Based on results for soils, we predicted a positive effect of OC content (Canarini et al., 2017) and a negative effect of the C/N ratio (Ramirez et al., 2012) and clay content (Borken & Matzner, 2009) on the response of respiration to rewetting. We also predicted positive effects of clay on OC content and of OC content on the C/N ratio (Rice, 2002). For distal drivers, we selected mean annual temperature and precipitation to describe climatic conditions, catchment land use (i.e., the percentage of agricultural plus urban areas) as a proxy of anthropogenic influence, and riparian plant cover and channel width to characterize stream features (Figure 2). We predicted that temperature, precipitation, land use and riparian cover indirectly affect the response of respiration to rewetting through their effects on OC content and the C/N ratio (Colman & Schimel, 2013; Raich & Potter, 1995). We also predicted a negative effect of land use and channel width on riparian cover (Naiman et al., 2005).

In the second step of the SEM approach, we used the maximum likelihood method to obtain a global estimation (Grace et al., 2012). Exploratory data analysis suggested the need to square-root transform or ln-transform the response variables (including respiration rates) and five explanatory variables (Code S1), to ensure linearity of relationships and, hence, the suitability of the global estimation method. The metamodel was fitted and tested by means of the function sem() in the R package *lavaan* (Rosseel, 2012). The user-friendly or minimalist approach was used because it provides an iterative process to confront all our initial assumptions with data, and because, after prior transformations of variables, non-standard models were not required (Code S1). Data to model discrepancy was evaluated by means of the function modindices() in the *lavaan* package (Code S1). This is an iterative process in which data to model consistency is assessed with a chi-square test comparing the tested models to a saturated model. The iterative process ended when the modindices() output indicated that no further meaningful modifications were possible and the null hypothesis of model consistency could not be rejected. Two goodness-of-fit measures, the comparative fit index (CFI) and the root mean square error of approximation (RMSEA), were also calculated. The final models were accepted when the *p*-value associated with the corresponding chi-square test was > 0.05, CFI > 0.95 and RMSE < 0.05 (Code S1).

Because changes in sediment respiration upon rewetting were measured with two methods (MicroResp™ and bottle incubation), the above SEM process was applied independently for the two response variables. Upon acceptance of a final SEM, the presence of residual spatial autocorrelation was tested using spatial correlograms (Moran's *I* statistic) with Holm's correction for multiple testing (Legendre & Legendre, 2012) (Code S1). Because no spatial autocorrelation was found in the residuals once the SEM processes ended, special spatial structures were not introduced. Finally, we explored partial effects fitted in the SEM using regressions between variables and model residuals for the main relationships.

3. Results and Discussion

3.1. Magnitude of Sediment Respiration

Sediment respiration in dry conditions (MicroResp™ method) ranged from 0.01 to 14.1 nmol CO_2 g^{-1} dry mass h^{-1} (mean ± SE = 1.1 ± 0.1, median = 0.8; Figure 3a; Table 1). These low respiration rates are similar to those reported from other ex situ dry stream sediments in earlier studies (0.2–4.5 nmol CO_2 g^{-1} dry mass h^{-1}; measured with the MicroResp™ method in dry conditions) (Gómez-Gener et al., 2015), and overall support results from soil studies showing a reduction in, but not full suppression of, respiration after

© 2019 American Geophysical Union. All rights reserved.

drying (Schimel, 2018). This indicates that dry IRES sediments, like soils, support a moderately active microbial community.

Sediment respiration increased upon rewetting, ranging from 0.01 to 147 nmol CO_2 g^{-1} dry mass h^{-1} (mean ± SE = 34.9 ± 4.7, median = 27.0) for the MicroResp™ method and from 0 to 411 nmol CO_2 g^{-1} dry mass h^{-1} (mean ± SE = 72.0 ± 4.7, median = 54.3) for the bottle incubations method (Figure 3a; Table 1). These values are in the upper range of respiration rates reported from perennial stream sediments (range = 0–356 nmol CO_2 g^{-1} dry mass h^{-1}, median = 19; Table S1), suggesting that rewetting events after dry phases in IRES are associated with rapid recovery of metabolic activity by heterotrophic organisms present in the sediments (Schimel, 2018). Comparison of our respiration rates with estimates of soil respiration are hampered by the different methods used to measure respiration in soils, and by the reporting of most rates on an areal basis (Kim et al., 2012). Nonetheless, a cross-European study of basal soil respiration measured with the MicroResp™ method at 60% water holding capacity reported similar values to ours (41.6–225 nmol CO_2 g^{-1} dry mass h^{-1}, n = 81) (Creamer et al., 2016), suggesting that respiration rates in IRES sediments upon rewetting are similar to those in mesic soils.

The much higher sediment respiration upon rewetting, with a mean 32-fold (MicroResp™) or 66-fold (bottle incubation) increase in wet compared to dry conditions (Figure 3a; Table 1), is in the upper range of increases reported after rewetting from both streams and soils. The CO_2 flux from soils can increase 0.4–130-fold (mean = 12) after rewetting, with the highest increases typically reported from deserts (Kim et al., 2012). Similarly, in dry IRES of the semiarid southwestern USA, the CO_2 flux increased 6–33-fold (mean = 19) immediately following experimental rewetting (Gallo et al., 2013). These findings point to the 'Birch effect' in IRES sediments, which is likely to result from microbial activity being stimulated by the rapid mobilization of nutrients and OC that accumulated during the dry phase, supplemented by newly available OC released during the disintegration of sediment aggregates and microbial cell lysis in response to osmotic stress upon rewetting (Borken & Matzner, 2009; Kim et al., 2012; Schimel, 2018).

The higher rates measured by bottle incubations compared to the MicroResp™ method (Figure 3a and b) were expected, because the bottle incubation assay simulates a typical reinundation event, whereas MicroResp™ simulates more moderate rewetting such as that caused by light rainfall. Nonetheless, the rates estimated with both methods were positively related to one another (Figure 3b), indicating they were interchangeable with respect to the mechanistic analyses of drivers of respiration response.

3.2. Drivers of Sediment Respiration

The SEM of sediment respiration change upon rewetting determined in bottle incubations supported the metamodel (Figure 4; Table S2). However, the final diagram depicting causal relationships (i.e., the paths linking the considered variables; Figure 4a) included just 10 paths and was thus more parsimonious than the metamodel. The final fitted model (Figure 4a) confirmed some of the predicted relationships (e.g., between riparian cover and land use) but not others (e.g., between land use and C/N ratio). In addition, we identified two unpredicted causal paths (between precipitation and riparian cover, and between clay content and the C/N ratio), increasing the overall model-to-data fit. In the final model output, 45% of the variance in sediment respiration change upon rewetting was explained by sediment OC content, the C/N ratio and clay content. In turn, OC content (R^2 = 30%) and the C/N ratio (R^2 = 13%) were explained by different combinations of proximal drivers (clay content) and distal drivers (riparian cover and temperature), and riparian cover (R^2 = 5%) was

© 2019 American Geophysical Union. All rights reserved.

explained by land use and precipitation (Figure 4a). The partial relationships fitted in the SEM were significant (Figure 4b, c and d). The same structure was obtained when respiration change upon rewetting determined with the MicroResp™ method was modelled, with the only major difference that overall R^2 = 21% instead of 45% (Table S3). The absolute β estimate values corresponding to the partial relationships also changed, but not their direction (Table S3). These results demonstrate how distal drivers (i.e., climate, land use and riparian cover) modulate proximal drivers (i.e., sediment texture, organic matter quantity and quality) to control sediment respiration upon rewetting in IRES.

The positive relationship between OC content and the respiration response to rewetting (Figure 4a) aligns with results from studies in rewetted stream sediments (Gallo et al., 2013) and soils (Kim et al., 2012), in which OC content and respiration or CO_2 release are typically positively related. This relationship held despite the low OC content of the sampled IRES sediments, which ranged from 0.1 to 8.5% (mean ± SE = 1.0 ± 0.1%, median = 0.5; Table 1). In a compilation of sediment chemistry data from perennial streams in the USA (Horowitz & Stephens, 2008), the OC content ranged from 0.01 to 28.7% (mean ± SE = 3.8 ± 0.1%, median = 2.7, n = 949), indicating that OC content in IRES sediments may be lower than in perennial streams. The dynamic hydrologic regime of IRES, which includes frequent flushing of accumulated material during periods of flow, may account for this difference (Arce et al., 2019). In an extensive survey of European topsoils (Tóth et al., 2013), OC contents ranged from 0.1 to 58.7% (mean ± SE = 4.9 ± 0.06%, median = 2.1, n = 19,969), which is also higher than in the studied IRES sediments, corroborating two previous comparisons of IRES sediments and soils within the same catchment (Boix-Fayos et al., 2015; Gómez-Gener et al., 2016). The lower OC content in dry IRES sediments compared to soils is likely to reflect geomorphological processes that form streambed sediments from eroded soils as well as the greater hydrological variability and lower biomass or lack of plants in IRES (Arce et al., 2019).

The negative relationship between the C/N ratio and sediment respiration upon rewetting (Figure 4a) matches previous observations in soils and could reflect the selection of microorganisms with copiotrophic life strategies (Fierer et al., 2007) under relatively nutrient-rich conditions (i.e., low C/N ratio) (Ramirez et al., 2012). These fast-growing organisms have high requirements for labile OC and nutrients (Fierer et al., 2007) and are expected to be less resistant but more resilient to environmental stresses such as rewetting (De Vries & Shade, 2013). Copiotrophic microorganisms may be responsible for the rapid reactivation of respiration observed upon rewetting, as they also thrive on labile OC and nutrients released by cell lysis upon rewetting (Schimel et al., 2007). Notably, the sediment C/N molar ratio measured in the sampled IRES was highly variable (mean ± SE = 26 ± 2.2, range = 2.4–211; Table 1), spanning, for instance, a wider range than samples in the European topsoil database (mean ± SE = 11.8 ± 0.04; range = 0.6–168, n = 19,952, data excluded where N content = 0%) (Tóth et al., 2013).

The negative relationship between clay content and respiration upon rewetting (Figure 4a) indicated greater respiration in coarser sediments. This result contrasts with findings in perennial streams, in which increases in sediment respiration with clay content have been linked to the increased surface area (Mendoza-Lera et al., 2017). In soils, however, high clay content favors compaction during drying and can delay OC mineralization by isolating microorganisms and adsorbing OC, which thus becomes less bioavailable upon rewetting (Borken & Matzner, 2009). Moreover, the indirect positive effect of clay content on respiration mediated by a decrease in the C/N ratio (Figure 4a) might be because higher clay content favors cation exchange capacity and nutrient retention (Bach et al., 2010). These results collectively suggest that upon rewetting, the influence of sediment texture on

© 2019 American Geophysical Union. All rights reserved.

respiration is similar to that observed in soils. Notably, these patterns emerged despite the lower, less variable clay content of sampled IRES sediments (mean ± SE = 5.9 ± 0.4%, range = 0–32; Table 1) compared to soils (mean ± SE = 18 ± 0.09%, range = 0–79, *n* = 19,969) (Tóth et al., 2013), the former being mainly formed by deposition and sorting processes during transport and characterized by a lack of stabilizing structures (e.g., biocrusts, vascular plants) (Arce et al., 2019; Boix-Fayos et al., 2015).

SEM results also indicated that the effect of OC content on respiration was partially regulated by distal drivers (Figure 4a). Specifically, OC content was related negatively to temperature and positively to riparian cover. The latter, in turn, was negatively related to land use and positively to precipitation. The negative relationship between sediment OC content and temperature may reflect reduced C mineralization rates in both soils and stream sediments in colder regions, favoring OC accumulation in dry IRES sediments (Conant et al., 2011). The positive relationship between OC content and riparian cover indicates a key role of riparian plant litter as an OC source in IRES sediments (Datry et al., 2018), with land use and precipitation only indirectly related to sediment OC content via their effects on riparian cover. Thus, streams in catchments with lower anthropogenic influence and higher precipitation tended to have greater riparian cover, leading to higher sediment OC content and respiration. Channel width had no effect on sediment respiration either directly or indirectly via riparian cover (i.e., reduced OC inputs from riparian vegetation in wider streams), suggesting that respiration upon rewetting is independent of channel width and only partially depends on riparian vegetation. Other sources of OC in dry IRES sediments may include organic matter imported from upland and upstream as well as autochthonous sources (e.g., macrophyte remnants, periphyton) (von Schiller et al., 2017). However, these results are inconclusive, because the studied IRES reaches were mostly located in low-order streams with narrow channels and high riparian cover (Table 1).

The magnitude and drivers of sediment respiration pulses upon rewetting reported in this study should be viewed with caution, because respiration was measured in small samples, disconnected from their structural matrix, and under standardized laboratory conditions. For instance, the incubation temperature and the nutrient concentration in the water used for rewetting may have differed from those found at ambient conditions at the sampling sites. Nonetheless, our rates were obtained using two alternative methods, which we suggest effectively determined the effect of rewetting and allowed us to compare responses among sediments with different intrinsic properties. A substantial proportion of the variance in sediment respiration change upon rewetting remained unexplained in our SEM, suggesting some important drivers were not characterized. These may include sediment properties such as phosphorus content or microbial biomass and distal drivers such as the time since the last rewetting event. We encourage researchers to conduct more in situ rewetting experiments across multiple IRES and to measure these additional variables to corroborate and expand our observations.

3.3. Potential Contribution to CO_2 Emissions from the Global Stream Network

Our results suggest that the high sediment respiration rates in IRES upon rewetting may significantly contribute to CO_2 emissions from the global stream network. We estimated a mean (range) release rate from rewetted sediments of 10.0 (0.0–56.9) g C m^{-2} day^{-1}. These rates greatly exceed the release rates from rewetted leaf litter collected from the same IRES sites (mean = 0.24 g C m^{-2} day^{-1}, range = 0–3.7) (Datry et al., 2018), suggesting that sediments are key contributors to CO_2 emissions. A global upscaling of this release rate resulted in a mean (range) global CO_2 flux from a single rewetting in IRES sediments of 0.0045 (0.000–0.025) Pg C yr^{-1}, representing 4% (0–21%) of the global CO_2 emissions from

© 2019 American Geophysical Union. All rights reserved.

dry IRES (0.124 Pg C year^{-1} according to Marcé et al. [2019]) and between 0.2% (0.0–1.4%) and 0.8% (0.0–4.5%) of the global CO_2 emissions from perennial streams (0.56–1.8 Pg C yr^{-1} according to Aufdenkampe et al. [2011] and Raymond et al. [2013], respectively). Thus, a single respiration pulse resulting from rewetting of IRES sediments could increase annual CO_2 emissions from the global stream network, including IRES and perennial streams, by on average 0.2–0.7%.

The estimated contribution of respiration in IRES sediments upon rewetting to CO_2 emissions from the global stream network reported here may initially seem small. However, our estimate is conservative because the IRES surface area on which our calculations are based is likely an underestimate (Benstead & Leigh, 2012; Datry et al., 2018), IRES are often subject to multiple rewetting events (i.e., due to rain and flow reconnection) per year (Corti & Datry, 2012; Jacobson et al., 2000; von Schiller et al., 2017), and other processes also contribute to CO_2 emissions from IRES. For example, processes not recognized in our estimates include respiration in other stream compartments, such as plant litter and deeper sediments (Datry et al., 2018), and abiotic processes such as physical displacement and carbonate weathering (Marcé et al., 2019).

Although it is uncertain how well our laboratory-derived respiration rates scale to the natural environment, our results suggest that emissions from IRES during rewetting episodes may be a dominant term in the annual CO_2 balance in many stream networks where IRES and rewetting episodes are frequent. In any case, we are far from producing a robust global estimate of CO_2 emissions from IRES during rewetting events, because our calculations rely on several assumptions that need to be considered with caution: sediment densities are highly spatially variable (Boix-Fayos et al., 2015), respiration rates may change with sediment depth (Fang & Moncrieff, 2005), and the number of rewetting events varies greatly in space and time (von Schiller et al., 2017). Future research is needed to clarify the relevance of these uncertainties and processes, including the influence of antecedent flow conditions and type of rewetting (i.e., fed by groundwater, surface water or rainwater) on respiration response to rewetting.

4. Conclusions

Our global study, spanning 200 IRES reaches across six continents and covering a wide range of environmental conditions, enabled us to assess the magnitude and environmental drivers of respiration pulses in IRES sediments upon rewetting. Our data indicate that rewetting greatly increases sediment respiration, supporting the view of IRES as coupled aquatic-terrestrial ecosystems that function as 'punctuated biogeochemical reactors' in response to spatiotemporal fluctuations in drying and rewetting (Larned et al., 2010). The results also demonstrate that key sediment properties drive the response of respiration to rewetting, and, in turn, are influenced by climate and catchment conditions. Specifically, we found that organic-rich, low C/N and coarse sediments experience a larger respiration pulse upon rewetting, with greater riparian cover in more natural and humid catchments leading to higher respiration pulses by increasing the sediment OC content. These results expand our understanding of metabolism and C cycling in stream networks with implications for large-scale modelling efforts (Bernhardt et al., 2018). Furthermore, our findings support research demonstrating that rewetting events represent 'hot moments' (McClain et al., 2003) or 'control points' (Bernhardt et al., 2017) of CO_2 release in IRES, that is, short periods of high biogeochemical activity that may contribute significantly to the emissions of CO_2 from the global stream network. An update of respiration and CO_2 emissions in the global stream network is therefore needed, especially because the spatial extent of IRES and the frequency

© 2019 American Geophysical Union. All rights reserved.

of wetting-drying cycles is increasing due to climate change and other anthropogenic pressures.

Acknowledgments and Data

We thank Y. Etxeberria, L. Sánchez, C. Gutiérrez, G. LeGoff and B. Launay for laboratory support. DvS was supported by a Short-Term Scientific Mission of the COST Action CA15113 (SMIRES, Science and Management of Intermittent Rivers and Ephemeral Streams, www.smires.eu), supported by COST (European Cooperation in Science and Technology) and received additional funding from the EU's 7th Framework Programme for research, technological development and demonstration under grant agreement No. 603629 (GLOBAQUA) and a Grant for Research Groups of the Basque University System (IT-951-16) funded by the Basque Government. RM and BO were supported by the Spanish Ministry of Science, Innovation and Universities through project C-HYDROCHANGE (CGL2017-86788-C3-2-P and CGL2017-86788-C3-3-P). FA was funded by the Swiss National Science Foundation grants No. PP00P3_150698 and PP00P3_179089. NC was supported by the EU project LIFE+ TRivers (LIFE13 ENV/ES/000341). SDL received funding from the EU's Horizon 2020 research and innovation programme under the Marie Sklodowska-Curie grant agreement No 748625. PP and MP were supported by INTER-COST project LTC17017. The authors declare that they have no competing interests. The dataset (Data File S1; DOI: 10.6084/m9.figshare.8863721) and the R code used to generate the results (Code S1; DOI: 10.6084/m9.figshare.8863655), including step by step explanations of the statistical tests, have been deposited in Figshare Digital Repository (https://figshare.com/projects/Sediment_Respiration_Pulses_in_Intermittent_Rivers_and_Ephemeral_Streams/66104).

Author contributions: TD, AF, RC, DvS, and KT were responsible for project planning and project coordination. All authors collected sediments in their countries and processed this material. DvS, RM, BO and AE were responsible for laboratory analyses. RC, CML and DvS carried out the data compilation and database management. GGB, IO and DvS performed the data analyses. DvS led the writing of the manuscript with notable contributions by TD, AF, KT, RM, GGB, IO, BO, AE, CML, MOG and RS. All the other authors commented on and contributed to revising draft versions.

References

Acuña, V., Datry, T., Marshall, J., Barceló, D., Dahm, C. N., Ginebreda, A., et al. (2014). Why should we care about temporary waterways? *Science*, *343*, 1080–1081. https://doi.org/10.1126/science.1246666

Arce, M. I., Mendoza-Lera, C., Almagro, M., Catalan, N., Mutz, M., Romani, A., et al. (2019). A conceptual framework for understanding the biogeochemistry of dry riverbeds through the lens of soil science. *Earth-Science Reviews*, *188*, 441–453. https://doi.org/https://doi.org/10.1016/j.earscirev.2018.12.001

Arriaga, F. J., Lowery, B., & Mays, M. D. (2006). A fast method for determining soil particle size distribution using a laser instrument. *Soil Science*, *171*(9), 663–674. https://doi.org/10.1097/01.ss.0000228056.92839.88

Aufdenkampe, A. K., Mayorga, E., Raymond, P. A., Melack, J. M., Doney, S. C., Alin, S. R., et al. (2011). Riverine coupling of biogeochemical cycles between land, oceans, and atmosphere. *Frontiers in Ecology and the Environment*, *9*(1), 53–60. https://doi.org/10.1890/100014

© 2019 American Geophysical Union. All rights reserved.

Bach, E. M., Baer, S. G., Meyer, C. K., & Six, J. (2010). Soil texture affects soil microbial and structural recovery during grassland restoration. *Soil Biology and Biochemistry*, *42*(12), 2182–2191. https://doi.org/https://doi.org/10.1016/j.soilbio.2010.08.014

Bear, J. (1988). *Dynamics of fluids in porous media*. New York, NY, USA: Courier Corporation.

Benstead, J. P., & Leigh, D. S. (2012). An expanded role for river networks. *Nature Geosci*, *5*(10), 678–679. https://doi.org/10.1038/ngeo1593

Bernhardt, E. S., Blaszczak, J. R., Ficken, C. D., Fork, M. L., Kaiser, K. E., & Seybold, E. C. (2017). Control points in ecosystems: moving beyond the hot spot hot moment concept. *Ecosystems*, *20*(4), 665–682. https://doi.org/https://doi.org/10.1007/s10021-016-0103-y

Bernhardt, E. S., Heffernan, J. B., Grimm, N. B., Stanley, E. H., Harvey, J. W., Arroita, M., et al. (2018). The metabolic regimes of flowing waters. *Limnology and Oceanography*, *63*(S1), S99–S118. https://doi.org/https://doi.org/10.1002/lno.10726

Boix-Fayos, C., Nadeu, E., Quiñonero, J. M., Mart\'\inez-Mena, M., Almagro, M., & De Vente, J. (2015). Sediment flow paths and associated organic carbon dynamics across a Mediterranean catchment. *Hydrology and Earth System Sciences*, *19*(3), 1209. https://doi.org/https://doi.org/10.5194/hess-19-1209-2015

Borken, W., & Matzner, E. (2009). Reappraisal of drying and wetting effects on C and N mineralization and fluxes in soils. *Global Change Biology*, *15*(4), 808–824. https://doi.org/https://doi.org/10.1111/j.1365-2486.2008.01681.x

Canarini, A., Kiær, L. P., & Dijkstra, F. A. (2017). Soil carbon loss regulated by drought intensity and available substrate: a meta-analysis. *Soil Biology and Biochemistry*, *112*, 90–99. https://doi.org/https://doi.org/10.1016/j.soilbio.2017.04.020

Colman, B. P., & Schimel, J. P. (2013). Drivers of microbial respiration and net N mineralization at the continental scale. *Soil Biology and Biochemistry*, *60*, 65–76. https://doi.org/https://doi.org/10.1016/j.soilbio.2013.01.003

Conant, R. T., Ryan, M. G., Agren, G. I., Birge, H. E., Davidson, E. A., Eliasson, P. E., et al. (2011). Temperature and soil organic matter decomposition rates - synthesis of current knowledge and a way forward. *Global Change Biology*, *17*(11), 3392–3404. https://doi.org/10.1111/j.1365-2486.2011.02496.x

Corti, R., & Datry, T. (2012). Invertebrates and sestonic matter in an advancing wetted front travelling down a dry river bed (Albarine, France). *Freshwater Science*, *31*(4), 1187–1201. https://doi.org/10.1899/12-017.1

Creamer, R. E., Stone, D., Berry, P., & Kuiper, I. (2016). Measuring respiration profiles of soil microbial communities across Europe using MicroResp™ method. *Applied Soil Ecology*, *97*(Supplement C), 36–43. https://doi.org/10.1016/j.apsoil.2015.08.004

Datry, T., Foulquier, A., Corti, R., von Schiller, D., Tockner, K., Mendoza-Lera, C., et al. (2018). A global analysis of terrestrial plant litter dynamics in non-perennial waterways. *Nature Geoscience*, *11*, 497–503. https://doi.org/10.1038/s41561-018-0134-4

Döll, P., & Schmied, H. M. (2012). How is the impact of climate change on river flow regimes related to the impact on mean annual runoff? A global-scale analysis. *Environmental Research Letters*, *7*(1), 14037. https://doi.org/10.1088/1748-9326/7/1/014037

Fang, C., & Moncrieff, J. B. (2005). The variation of soil microbial respiration with depth in

© 2019 American Geophysical Union. All rights reserved.

relation to soil carbon composition. *Plant and Soil*, *268*(1), 243–253. https://doi.org/10.1007/s11104-004-0278-4

Fierer, N., Bradford, M. A., & Jackson, R. B. (2007). Toward an ecological classification of soil bacteria. *Ecology*, *88*(6), 1354–1364. https://doi.org/https://doi.org/10.1890/05-1839

Gallo, E. L., Lohse, K. A., Ferlin, C. M., Meixner, T., & Brooks, P. D. (2013). Physical and biological controls on trace gas fluxes in semi-arid urban ephemeral waterways. *Biogeochemistry*, *121*, 189–207. https://doi.org/10.1007/s10533-013-9927-0

Gómez-Gener, L., Obrador, B., von Schiller, D., Marcé, R., Casas-Ruiz, J. P., Proia, L., et al. (2015). Hot spots for carbon emissions from Mediterranean fluvial networks during summer drought. *Biogeochemistry*, *125*(3), 409–426. https://doi.org/10.1007/s10533-015-0139-7

Gómez-Gener, Lluís, Obrador, B., Marcé, R., Acuña, V., Catalán, N., Casas-Ruiz, J. P., et al. (2016). When water vanishes: magnitude and regulation of carbon dioxide emissions from dry temporary streams. *Ecosystems*, *19*(4), 710–723. https://doi.org/https://doi.org/10.1007/s10021-016-9963-4

Gordon, N. D., McMahon, T. A., & Finlayson, B. L. (2004). *Stream Hydrology: an Introduction for Ecologists*. West Sussex, UK: Wiley.

Grace, J. B., Schoolmaster, D. R., Guntenspergen, G. R., Little, A. M., Mitchell, B. R., Miller, K. M., & Schweiger, E. W. (2012). Guidelines for a graph-theoretic implementation of structural equation modeling. *Ecosphere*, *3*(8), 1–44. https://doi.org/https://doi.org/10.1890/ES12-00048.1

Hillel, D. (1980). *Fundamentals of Soil Physics*. New York, NY, USA: Academic Press.

Horowitz, A. J., & Stephens, V. C. (2008). The effects of land use on fluvial sediment chemistry for the conterminous U.S. — Results from the first cycle of the NAWQA Program: Trace and major elements, phosphorus, carbon, and sulfur. *Science of The Total Environment*, *400*(1), 290–314. https://doi.org/https://doi.org/10.1016/j.scitotenv.2008.04.027

Jacobson, P. J., Jacobson, K. M., Angermeier, P. L., & Cherry, D. S. (2000). Variation in material transport and water chemistry along a large ephemeral river in the Namib Desert. *Freshwater Biology*, *44*(3), 481–491. https://doi.org/10.1046/j.1365-2427.2000.00604.x

Kim, D. G., Vargas, R., Bond-Lamberty, B., & Turetsky, M. R. (2012). Effects of soil rewetting and thawing on soil gas fluxes: A review of current literature and suggestions for future research. *Biogeosciences*, *9*(7), 2459–2483. https://doi.org/10.5194/bg-9-2459-2012

Larned, S. T., Datry, T., Arscott, D. B., & Tockner, K. (2010). Emerging concepts in temporary-river ecology. *Freshwater Biology*, *55*(4), 717–738. https://doi.org/10.1111/j.1365-2427.2009.02322.x

Legendre, P., & Legendre, L. F. J. (2012). *Numerical ecology*. Amsterdam, The Netherlands: Elsevier, Amsterdam.

Leopold, L. B. (1966). *Channel and Hillslope Processes in a Semiarid Area, New Mexico*. US Department of the Interior, Washington DC.

Marcé, R., Obrador, B., Gómez-Gener, L., Catalán, N., Koschorreck, M., Arce, M. I., et al. (2019). Emissions from dry inland waters are a blind spot in the global carbon cycle.

© 2019 American Geophysical Union. All rights reserved.

Accepted Article

Earth-Science Reviews, *188*, 240–248. https://doi.org/https://doi.org/10.1016/j.earscirev.2018.11.012

McClain, M. E., Boyer, E. W., Dent, C. L., Gergel, S. E., Grimm, N. B., Groffman, P. M., et al. (2003). Biogeochemical hot spots and hot moments at the interface of terrestrial and aquatic ecosystems. *Ecosystems*, *6*(4), 301–312. https://doi.org/https://doi.org/10.1007/s10021-003-0161-9

Mendoza-Lera, C., Frossard, A., Knie, M., Federlein, L. L., Gessner, M. O., & Mutz, M. (2017). Importance of advective mass transfer and sediment surface area for streambed microbial communities. *Freshwater Biology*, *62*(1), 133–145. https://doi.org/https://doi.org/10.1111/fwb.12856

Naiman, R. J., Decamps, H., & McClain, M. E. (2005). *Riparia: Ecology, Conservation, and Management of Streamside Communities*. London, UK: Elsevier, London.

Pinheiro, J., Bates, D., DebRoy, S., & Sarkar, D. (2016). nlme: Linear and Nonlinear Mixed Effects Models. R package version 3.1-128.

Pistocchi, A., Bouraoui, F., & Bittelli, M. (2008). A simplified parameterization of the monthly topsoil water budget. *Water Resources Research*, *44*(12), W12440. https://doi.org/10.1029/2007WR006603

Pumo, D., Caracciolo, D., Viola, F., & Noto, L. V. (2016). Climate change effects on the hydrological regime of small non-perennial river basins. *Science of The Total Environment*, *542*, 76–92. https://doi.org/https://doi.org/10.1016/j.scitotenv.2015.10.109

R Core Team. (2016). R: A Language and Environment for Statistical Computing. R Foundation for Statistical Computing, version 3.3.1 Vienna, Austria. Vienna, Austria.

Raich, J. W., & Potter, C. S. (1995). Global patterns of carbon dioxide emissions from soils. *Global Biogeochemical Cycles*, *9*(1), 23–36. https://doi.org/10.1029/94GB02723

Ramirez, K. S., Craine, J. M., & Fierer, N. (2012). Consistent effects of nitrogen amendments on soil microbial communities and processes across biomes. *Global Change Biology*, *18*(6), 1918–1927. https://doi.org/https://doi.org/10.1111/j.1365-2486.2012.02639.x

Raymond, P. A., Hartmann, J., Lauerwald, R., Sobek, S., McDonald, C., Hoover, M., et al. (2013). Global carbon dioxide emissions from inland waters. *Nature*, *503*(7476), 355–359. https://doi.org/10.1038/nature12760

Rice, C. W. (2002). Organic matter and nutrient dynamics. In R. Lal (Ed.), *Encyclopedia of Soil Science* (2nd ed., pp. 1180–1183). New York, NY, USA: Marcel Dekker, New York.

Rosseel, Y. (2012). Lavaan: An R package for structural equation modeling. *Journal of Statistical Software*, *48*, 1–36.

von Schiller, D., Bernal, S., Dahm, C. N., & Martí, E. (2017). Nutrient and Organic Matter Dynamics in Intermittent Rivers and Ephemeral Streams. In Thibault Datry, N. Bonada, & A. J. Boulton (Eds.), *Intermittent Rivers and Ephemeral Streams* (pp. 135–160). Cambridge, MA, USA: Academic Press.

Schimel, J. P. (2018). Life in dry soils: effects of drought on soil microbial communities and processes. *Annual Review of Ecology, Evolution, and Systematics*, *49*(1), 409–432. https://doi.org/10.1146/annurev-ecolsys-110617-062614

Schimel, J. P., Balser, T. C., & Wallenstein, M. (2007). Microbial stress-response physiology and its implications for ecosystem function. *Ecology*, *88*(6), 1386–1394.

© 2019 American Geophysical Union. All rights reserved.

Accepted Article

https://doi.org/https://doi.org/10.1890/06-0219

Tóth, G., Jones, A., & Montanarella, L. (2013). The LUCAS topsoil database and derived information on the regional variability of cropland topsoil properties in the European Union. *Environmental Monitoring and Assessment*, *185*(9), 7409–7425. https://doi.org/https://doi.org/10.1007/s10661-013-3109-3

De Vries, F. T., & Shade, A. (2013). Controls on soil microbial community stability under climate change. *Frontiers in Microbiology*, *4*, 265. https://doi.org/https://doi.org/10.3389/fmicb.2013.00265

Accepted Article

© 2019 American Geophysical Union. All rights reserved.

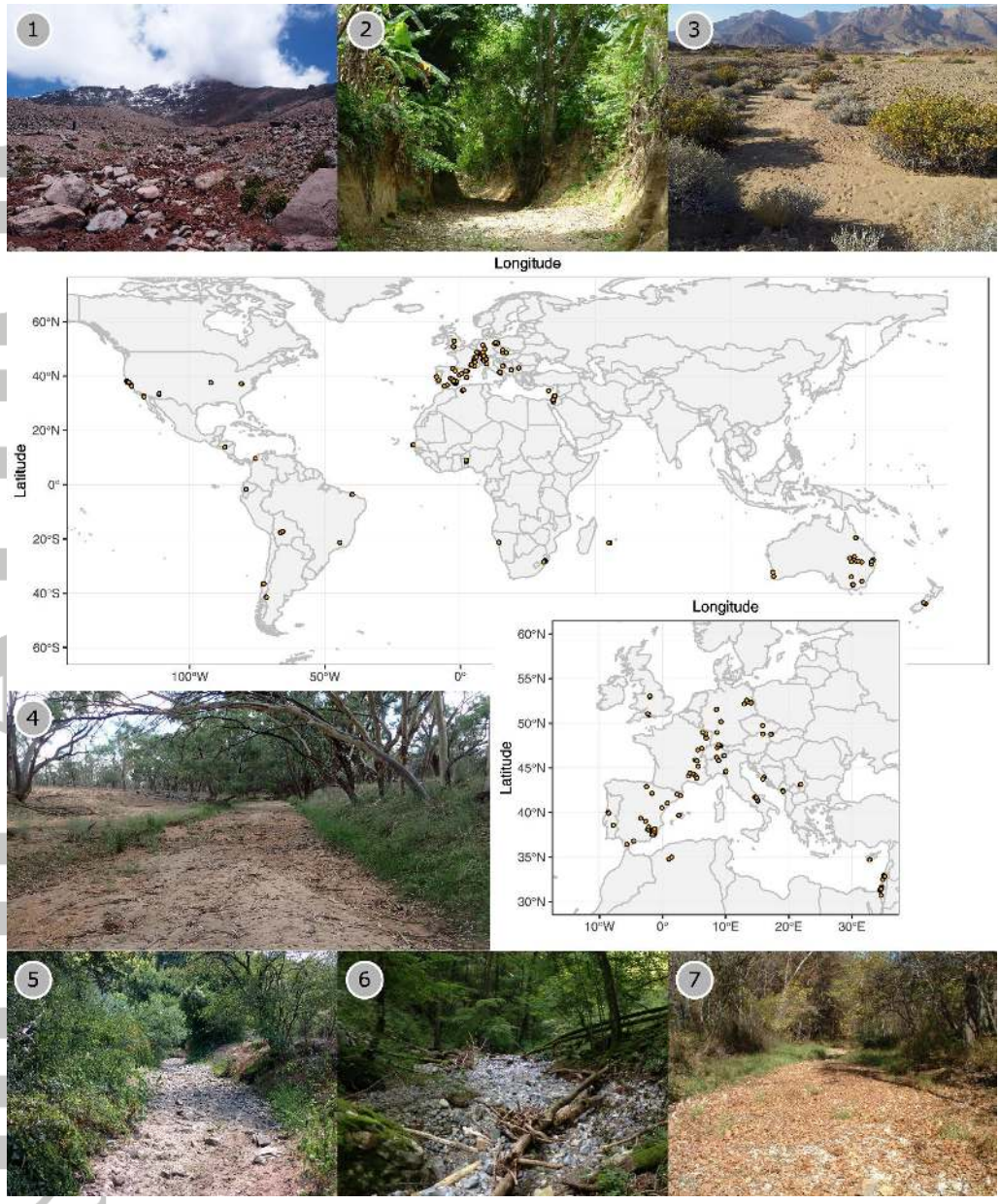

Figure 1. Global distribution of the sampling sites and photos of selected sites. The 200 sampled dry stream reaches were in 29 countries on six continents and encompassed a wide range of environmental conditions. The inset illustrates the spatial distribution within the most densely sampled area. Photos are shown for a high mountain stream in Ecuador (1), a tropical stream in Colombia (2), a desert stream in Namibia (3), a semiarid stream in Australia (4), and for temperate forested streams in Serbia (5), Switzerland (6) and the USA (7). Photo credits: 1: S. Cauvy-Fraunié, IRSTEA, France. 2: J. F. Blanco-Libreros, Universidad de Antioquia, Colombia. 3: M. Moleón, University of Granada, Spain. 4: P. Negus, Queensland Government, Australia. 5: A. Savić, University of Niš, Serbia. 6: A. Bruder, University of Applied Sciences and Arts of Southern Switzerland, Switzerland. 7: D. Niyogi, Missouri University of Science and Technology, USA.

Accepted Article

© 2019 American Geophysical Union. All rights reserved.

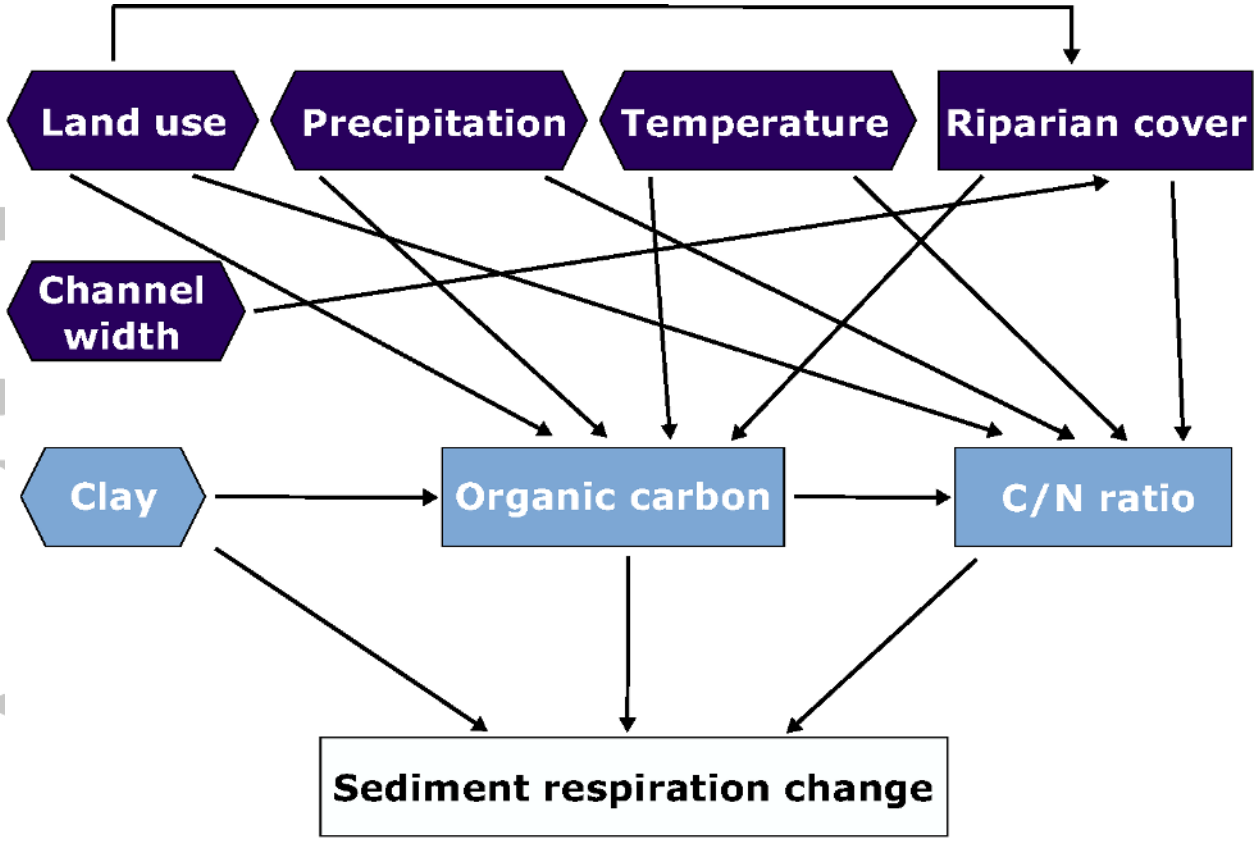

Figure 2. Metamodel showing all predicted connections among variables potentially driving sediment respiration change upon rewetting. Dark-blue frames and light-blue frames indicate distal and proximal drivers, respectively. The white frame represents the response variable. Hexagons and rectangles indicate exogenous and endogenous variables, respectively.

Accepted

© 2019 American Geophysical Union. All rights reserved.

Accepted Article

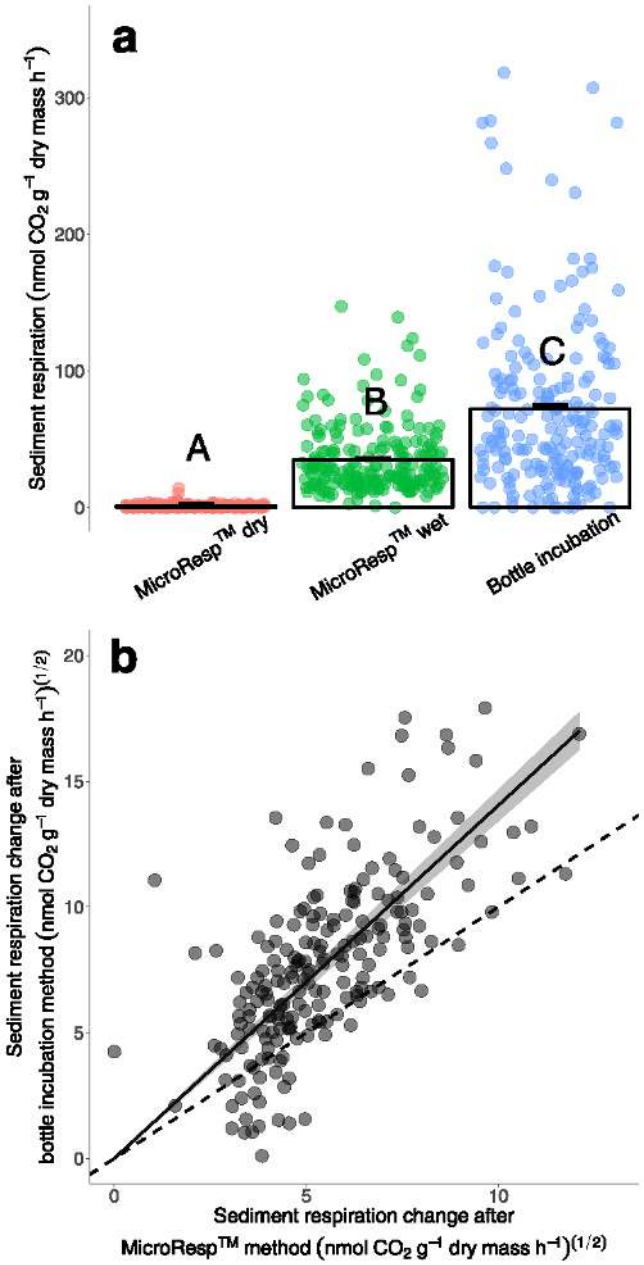

Figure 3. Sediment respiration in dry and rewetted conditions. (a) Mean + SE of sediment respiration in three types of standardized assays. Differences between types are significant (ANOVA, $F_{2, 398} = 748.6$, $p < 0.001$). Upper case letters denote significant differences as determined by Tukey's post hoc comparisons ($p < 0.001$). (b) Relationship between changes in respiration upon sediment rewetting as measured with the MicroResp™ and bottle incubation methods ($F_{1,199} = 1993.3$, $p < 0.001$, $R^2 = 48.5\%$). The grey area indicates the 95% confidence interval for the regression line. The slope of the regression line is significantly different from the 1:1 line (dashed line; $t_{199} = 12.9$, $p < 0.001$), indicating that the bottle incubation method tends to produce higher sediment respiration rates than the MicroResp™ method. Note the square root transformation of both axes.

© 2019 American Geophysical Union. All rights reserved.

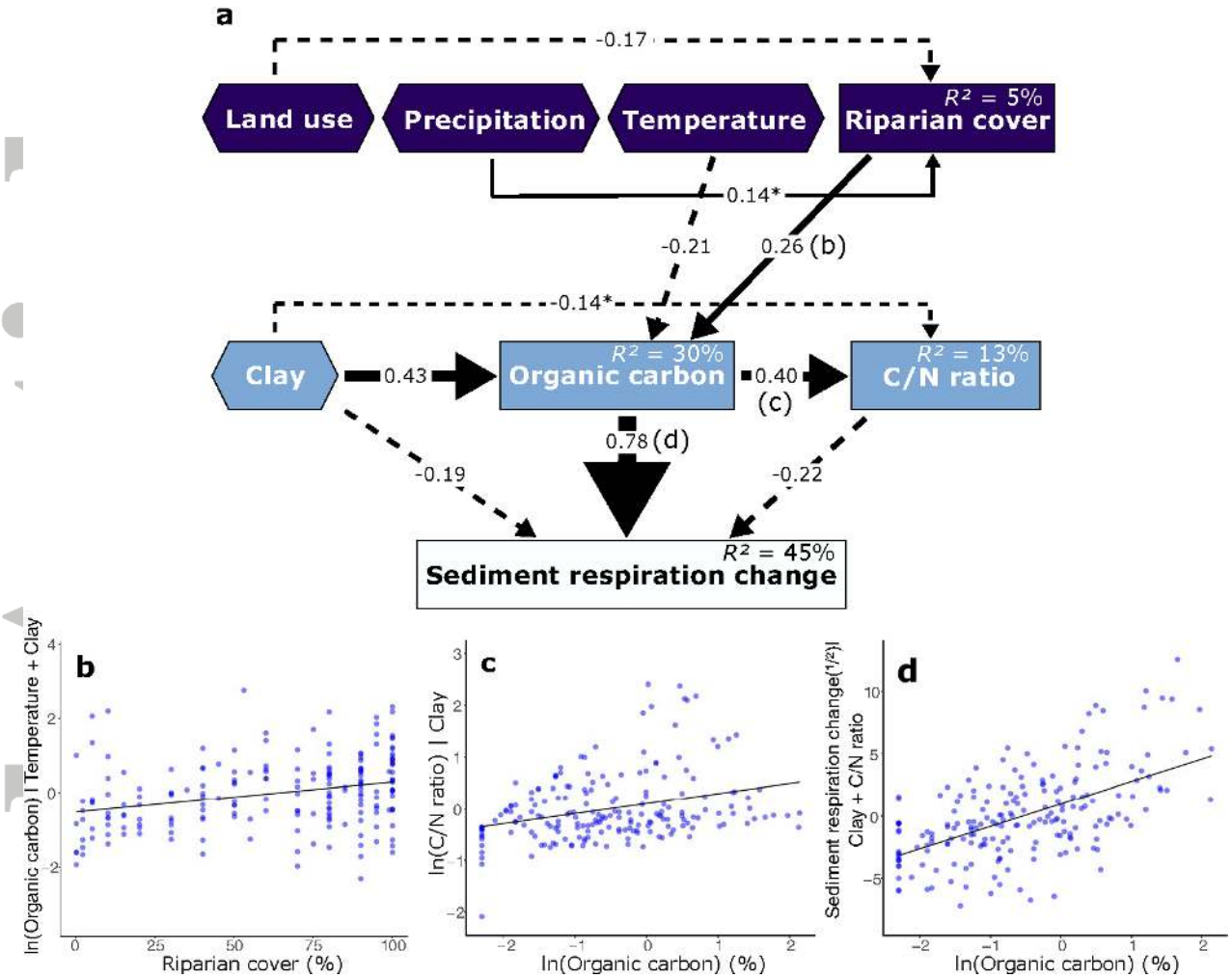

Figure 4. Drivers of sediment respiration change upon rewetting. (a) Final accepted structural equation model (SEM) showing all significant connections supported by the bottle incubation data ($\chi^2(12, n = 200) = 13.3$; $p = 0.35$, CFI = 0.99, RMSEA = 0.023). The white frame represents the response variable. Hexagons and rectangles indicate exogenous and endogenous variables, respectively. Solid arrows and dashed arrows indicate positive and negative relationships, respectively. Numbers adjacent to arrows are the standardized effect sizes of the relationship (unstandardized coefficients are shown in Table S2). Arrow width is proportional to the strength of the effect size, and R^2 values denote the percentage of variance explained. Asterisks indicate relationship not included in the metamodel. (b, c and d) Linear regressions between variables and model residuals for the main relationships in the final SEM are indicated by matching letters in b ($z = 4.3$, $p < 0.001$ for c; $z = 5.4$, $p < 0.001$ for d; $z = 12.5$, $p < 0.001$ for e). Note the square root or ln transformation of some axes.

© 2019 American Geophysical Union. All rights reserved.

Accepted Article

Table 1. Descriptive statistics of environmental and sediment variables characterizing 200 globally distributed IRES. IQR = interquartile range; SE = standard error.

Variable	Description	Median	IQR	Mean	SE	Range
Riparian cover	Percentage area of the sampling reach covered by a plant canopy	75	56	62	2.4	0–100
Temperature	Mean annual temperature (°C)	13.8	7.8	14.1	0.4	-1.2–27.7
Precipitation	Mean annual precipitation (mm)	758	425	805	30	5–3469
Channel width	Active channel width (m)	3.0	2.9	3.5	0.2	0.3–13.5
Land use	Percentage of the catchment covered by urban and agricultural areas	45	69	46	3	0–100
Organic carbon	Sediment organic carbon content (%)	0.5	1.0	1.0	0.1	0.1–8.5
C/N ratio	Molar ratio of organic carbon to nitrogen in sediments	16.3	11.8	25.9	2.2	2.4–211.3
Clay	Percentage of sediment particles <2 µm	3.3	8.4	5.9	0.4	0.0–32.1

© 2019 American Geophysical Union. All rights reserved.